

Transparent PT-symmetric nonlinear networks

M.E. Akramov¹, J.R. Yusupov², M. Ehrhardt³, H. Susanto⁴ and D.U. Matrasulov⁵

¹National University of Uzbekistan, Universitet Str. 4, 100174, Tashkent, Uzbekistan

²Kimyo Int. University in Tashkent, 156 Usman Nasyr Str., 100121, Tashkent, Uzbekistan

³Bergische Universität Wuppertal, Gaußstrasse 20, D-42119 Wuppertal, Germany

⁴Khalifa University, 127788, Abu Dhabi, United Arab Emirates

⁵Turin Polytechnic University in Tashkent, 17 Niyazov Str., 100095, Tashkent, Uzbekistan

August 8, 2024

Abstract

We consider reflectionless wave propagation in networks modeled in terms of the nonlocal nonlinear Schrödinger (NNLS) equation on metric graphs, for which transparent boundary conditions are imposed at the vertices. By employing the “potential approach” previously used for the nonlinear Schrödinger equation, we derive transparent boundary conditions for the NNLS equation on metric graphs. These conditions eliminate backscattering at graph vertices, which is crucial for minimizing losses in signal, heat, and charge transfer in various applications such as optical fibers, optoelectronic networks, and low-dimensional materials.

AMS classification: 65M99, 81-08, 37N20

Keywords: NNLS equation, metric graphs, transparent boundary conditions, potential approach, nonlinear optics, ferromagnetic structures.

1 Introduction

Nonlocal nonlinear Schrödinger (NNLS) equation attracted much attention since its pioneering study by Ablowitz and Muslimani published in the Ref. [1], where they showed integrability of the problem and obtained a soliton solution. An interesting feature of the soliton solution of the NNLS equation obtained by Ablowitz and Muslimani is caused by its nonlocality, i.e. the solution at a point x_1 depends on the solution at point $-x_1$. Another important feature is the fact that the NNLS equation is PT-symmetric. Later, various aspects of the NNLS equation were studied in a series of papers by Ablowitz and Muslimani [2, 3, 4, 5, 6, 7] and other authors (see, e.g., Refs. [8, 9, 10, 11, 12, 13, 14]). Besides nonlocality and PT symmetry, the NNLS equation has practical importance from the viewpoint of practical applications in nonlinear optics and some ferromagnetic structures. Here we consider the problem of the NNLS equation on metric graphs with a focus on transparent vertex boundary conditions. The latter means the boundary conditions that ensure the absence of

backscattering at the graph vertex. To do this, we use the so-called ‘‘potential approach’’, which was previously used to impose transparent vertex boundary conditions for the nonlinear Schrödinger equation on metric graphs [15].

The motivation for the study of transparent boundary conditions in networks comes from their application in several technologically important problems, such as tunable soliton dynamics in branched optical fibers and optoelectronic networks, and the control of quasiparticle transport in low-dimensional branched functional materials. We note that evolution equations on metric graphs have attracted much attention in different context for past two decades [16, 17, 18, 19, 20, 21, 22, 23, 24, 25, 26]. In all these cases, it is necessary to reduce losses in signal, heat and charge transfer along the structure by constructing an appropriate network architecture.

The paper is organized as follows. In Section 2 we briefly introduce soliton solutions and conserving quantities for NNLS equation on a line and recall the main steps of deriving the transparent boundary conditions (TBCs). In Section 3 we derive TBCs for the NNLS equation on metric graphs. Section 4 demonstrates the verification of the obtained results by a numerical experiment. Finally, Section 5 contains the concluding remarks.

2 Transparent boundary conditions for the nonlocal nonlinear Schrödinger equation on a line

2.1 Soliton solutions of the nonlocal nonlinear Schrödinger equation

Let us consider the NNLS equation on a line

$$i\partial_t q(x, t) + \partial_x^2 q(x, t) + 2q(x, t)q^*(-x, t)q(x, t) = 0, \quad (1)$$

where q^* denotes the complex conjugate of q and the self-induced potential, which can be defined as $V(x, t) = 2q(x, t)q^*(-x, t)$, has the PT-symmetric property, i.e. $V(x, t) = V^*(-x, t)$. Note that the nonlocality of Eq. (1) arises from the term $q^*(-x, t)$ which implies that the solution $q(x, t)$ at coordinate x always requires information from the opposite point $-x$. For the above NNLS equation, there are many different types of soliton solutions, such as breathing, periodic, rational, and others. For example, a single soliton solution found by the inverse scattering method in Ref. [1] is written as:

$$q(x, t) = -\frac{2(\eta_1 + \bar{\eta}_1) e^{i\bar{\theta}_1} e^{4i\bar{\eta}_1^2 t} e^{-2\bar{\eta}_1 x}}{1 + e^{i(\theta_1 + \bar{\theta}_1)} e^{-4i(\eta_1^2 - \bar{\eta}_1^2)t} e^{-2(\eta_1 + \bar{\eta}_1)x}}, \quad (2)$$

with η_1 , $\bar{\eta}_1$, θ_1 , and $\bar{\theta}_1$ being real constants. An important feature of this soliton solution (2) is the fact that it describes a wave that looks like a ‘‘bird that flaps its wings but does not fly/move’’.

A traveling soliton solution of Eq. (1) derived in Ref. [8] is written as

$$q(x, t) = \frac{\alpha_1 e^{-\Delta/2} e^{i(\bar{\xi}_{1R} - \xi_{1R}) + i(\bar{\xi}_{1I} - \xi_{1I})}}{2[\cosh(\chi_1) \cos(\chi_2) + i \sinh(\chi_1) \sin(\chi_2)]}, \quad (3)$$

where $\chi_1 = (\xi_{1R} + \bar{\xi}_{1R} + \Delta_R)/2$, $\chi_2 = (\xi_{1I} + \bar{\xi}_{1I} + \Delta_I)/2$, $\xi_{1R} = -k_{1I}(x + 2k_{1R}t)$, $\xi_{1I} = k_{1R}x - (k_{1I}^2 - k_{1R}^2)t$, $\bar{\xi}_{1R} = -\bar{k}_{1I}(x + 2\bar{k}_{1R}t)$, $\bar{\xi}_{1I} = \bar{k}_{1R}x - (\bar{k}_{1R}^2 - \bar{k}_{1I}^2)t$,

$$\Delta_R = \log\left(\frac{|\alpha_1|^2 |\beta_1|^2}{|k_1 + \bar{k}_1|^2}\right), \quad \Delta_I = -\frac{i}{2} \log\left(\frac{\alpha_1 \beta_1 (k_1^* + \bar{k}_1^*)^2}{\alpha_1^* \beta_1^* (k_1 + \bar{k}_1)^2}\right), \quad \Delta = \log\left(-\frac{\alpha_1 \beta_1}{(k_1 + \bar{k}_1)^2}\right),$$

with α_1, β_1, k_1 and \bar{k}_1 are arbitrary complex constants, k_{1R}, \bar{k}_{1R} and k_{1I}, \bar{k}_{1I} are real and imaginary parts of k_1, \bar{k}_1 , respectively.

The integrability of the problem was proved in [1], which means that the NNLS equation has infinitely many conservation laws. In particular, two important conservation quantities, the norm and the energy, were derived in [1] and are as follows

$$\begin{aligned} N(t) &= \int_{-\infty}^{+\infty} q(x, t) q^*(-x, t) dx, \\ E(t) &= \int_{-\infty}^{+\infty} \left[\partial_x q(x, t) \cdot \partial_x q^*(-x, t) + q^2(x, t) \cdot q^{*2}(-x, t) \right] dx. \end{aligned} \tag{4}$$

The above soliton solutions of Eq. (1) are obtained assuming decay conditions at infinity, i.e. $q(x, t) \rightarrow 0$ for $x \rightarrow \pm\infty$.

2.2 Transparent boundary conditions

Here, following Ref. [27], we briefly recall the problem of transparent boundary conditions (TBCs) for the NNLS equation on a line, which is based on the use of the so-called *potential approach*, which was first proposed in [28]. The effectiveness of this approach in deriving TBCs for various nonlinear evolution equations has been shown in the Refs. [29, 30, 27]. Within the framework of this approach, the NNLS equation can be formally reduced to the linear Schrödinger equation

$$i\partial_t q(x, t) + \partial_x^2 q(x, t) + V(x, t)q(x, t) = 0, \tag{5}$$

with the potential $V(x, t) = 2q(x, t)q^*(-x, t)$. By introducing a new unknown $Q(x, t)$ given by the relation

$$Q(x, t) = e^{-i\mathcal{V}(x, t)} q(x, t), \tag{6}$$

with

$$\mathcal{V}(x, t) = \int_0^t V(x, s) ds, \tag{7}$$

we obtain the Schrödinger equation in terms of $Q(x, t)$ as

$$L(x, t, \partial_x, \partial_t)Q = i\partial_t Q + \partial_x^2 Q + A\partial_x Q + BQ = 0, \tag{8}$$

where $A = 2i\partial_x \mathcal{V}$ and $B = (i\partial_x^2 \mathcal{V} - (\partial_x \mathcal{V})^2)$. Using the pseudo-differential operator calculus [31] one can linearize Eq. (8) as

$$L = (\partial_x + i\Lambda^-)(\partial_x + i\Lambda^+) = \partial_x^2 + i(\Lambda^+ + \Lambda^-)\partial_x + i\text{Op}(\partial_x \lambda^+) - \Lambda^+ \Lambda^-, \tag{9}$$

where λ^+ is the principal symbol of the operator Λ^+ and $\text{Op}(p)$ denotes the associated operator of a symbol p . The Eqs. (8) and (9) lead to the system of operators

$$\begin{aligned} i(\Lambda^+ + \Lambda^-) &= A, \\ i\text{Op}(\partial_x \lambda^+) - \Lambda^+ \Lambda^- &= i\partial_t + B. \end{aligned} \tag{10}$$

Since the two functions A and B correspond to zero-order operators ($\text{Op}(a) = A$ and $\text{Op}(b) = B$), one obtains the symbolic system of equations as

$$\begin{aligned} i(\lambda^+ + \lambda^-) &= a, \\ i\partial_x \lambda^+ - \sum_{\alpha=0}^{+\infty} \frac{(-1)^\alpha}{\alpha!} \partial_\tau^\alpha \lambda^- \partial_t^\alpha \lambda^+ &= -\tau + b. \end{aligned} \quad (11)$$

An asymptotic evolution in the inhomogeneous symbols can be written as

$$\lambda^\pm \sim \sum_{j=0}^{+\infty} \lambda_{1/2-j/2}^\pm. \quad (12)$$

One can determine the $1/2$ -order terms in the first relation of the system (11) by substituting the expansion (12) into Eq. (11):

$$\lambda_{1/2}^- = -\lambda_{1/2}^+, \quad \lambda_{1/2}^+ = \pm\sqrt{-\tau}. \quad (13)$$

Here, the choice $\lambda_{1/2}^+ = \pm\sqrt{-\tau}$ corresponds to the Dirichlet-to-Neumann (DtN) operator. The system of equations for the zeroth-order terms can be written as

$$\begin{aligned} \lambda_0^- &= -\lambda_0^+ - ia, \\ i\partial_x \lambda_{1/2}^+ - (\lambda_0^- \lambda_{1/2}^+ + \lambda_0^+ \lambda_{1/2}^-) &= 0. \end{aligned} \quad (14)$$

Then, from Eq. (14) we obtain

$$\begin{aligned} \lambda_0^+ &= -i\frac{a}{2} = \frac{1}{2}\partial_x \mathcal{V}, \\ \lambda_0^- &= -\lambda_0^+ - ia = \frac{1}{2}\partial_x \mathcal{V}. \end{aligned} \quad (15)$$

Since $\partial_t^\alpha \lambda_{-1/2}^\pm = \partial_\tau^\alpha \lambda_0^\pm = 0$, $\alpha \in \mathbb{N}$, for the terms of order $-1/2$ we get

$$\begin{aligned} i(\lambda_{-1/2}^+ + \lambda_{-1/2}^-) &= 0, \\ i\partial_x \lambda_0^+ - (\lambda_{-1/2}^- \lambda_{1/2}^+ + \lambda_0^+ \lambda_0^- + \lambda_{-1/2}^+ \lambda_{1/2}^-) &= b. \end{aligned} \quad (16)$$

From Eq. (16) we obtain

$$\lambda_{-1/2}^\pm = 0. \quad (17)$$

In the same way one can obtain the terms of the next order as

$$\lambda_{-1}^- = -\lambda_{-1}^+, \quad \lambda_{-1}^+ = i\frac{\partial_x V}{4\tau}. \quad (18)$$

As a result, TBCs were derived up to the second-order approximation:

$$\partial_x q|_{x=-L} - e^{-i\frac{\pi}{4}} e^{i\nu} \partial_t^{1/2} (e^{-i\nu} q)|_{x=-L} - i\frac{\partial_x V}{4} e^{i\nu} I_t (e^{-i\nu} q)|_{x=-L} = 0, \quad (19a)$$

$$\partial_x q|_{x=L} + e^{-i\frac{\pi}{4}} e^{i\nu} \partial_t^{1/2} (e^{-i\nu} q)|_{x=L} + i\frac{\partial_x V}{4} e^{i\nu} I_t (e^{-i\nu} q)|_{x=L} = 0. \quad (19b)$$

where the operator $\partial_t^{1/2}$, which denotes the half-order fractional time derivative operator, is defined as

$$(\partial_t^{1/2} f)(t) = \frac{1}{\sqrt{\pi}} \partial_t \int_0^t \frac{f(s)}{\sqrt{t-s}} ds, \quad (20)$$

and the operator $I_t(f)$ is

$$(I_t f)(t) = \int_0^t f(s) ds. \quad (21)$$

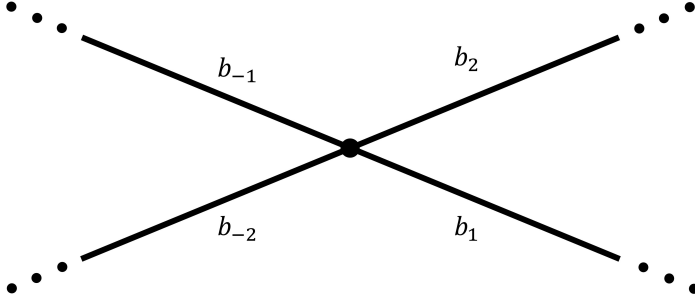


Figure 1: The simplest symmetric star graph with four bonds.

3 Transparent boundary conditions for the nonlocal nonlinear Schrödinger equation on metric graphs

3.1 Nonlocal nonlinear Schrödinger equation on a star graph

One of the restrictions on the class of initial conditions for NNLSE is that they must be even (in x), which makes the initial data symmetric with respect to the y -axis. Taking this property into account, we consider the simplest possible star graph with an even number of bonds (see, Fig. 1). The nonlocal nonlinear Schrödinger equation is written on each bond of the star graph with bonds $b_{\pm j}$ to which a coordinate $x_{\pm j}$ is assigned. We choose the origin of the coordinates at the vertex so that the bond b_{-j} takes values $x_{-j} \in (-\infty, 0)$ and for b_j we fix $x_j \in [0, +\infty)$:

$$i\partial_t q_{\pm j}(x, t) + \partial_x^2 q_{\pm j}(x, t) + \sqrt{\beta_j \beta_{-j}} q_{\pm j}^2(x, t) q_{\mp j}^*(-x, t) = 0, \quad (22)$$

where $q_{\pm j}(x, t)$ are defined in $x \in b_{\pm j}$, and $j = 1, 2$.

The Eq. (22) is a system of NLS equations where components of $q_{\pm j}$ are mixed in the nonlinear term due to the presence of the factor $\sqrt{\beta_j \beta_{-j}}$. To solve this equation, it is necessary to impose boundary conditions at the branching point (vertex) of the graph. Here we choose the boundary conditions derived in [32], which ensure that the considered system is integrable, and they are derived by showing that there exists an infinite number of conservation laws. Within this approach for the above NNLSE, the norm is determined as, cf. [1]

$$N(t) = \sum_{j=1}^2 [N_j(t) + N_{-j}(t)], \quad N_{\pm j}(t) = \int_{b_{\pm j}} q_{\pm j}(x, t) q_{\mp j}^*(-x, t) dx. \quad (23)$$

Another conserving quantity, i.e., the energy, is given by

$$E(t) = \sum_{j=1}^2 [E_j(t) + E_{-j}(t)], \quad E_{\pm j}(t) = \int_{b_{\pm j}} \left(\partial_x q_{\pm j}(x, t) \cdot \partial_x q_{\mp j}^*(-x, t) + \frac{\sqrt{\beta_j \beta_{-j}}}{2} q_{\pm j}^2(x, t) \cdot q_{\mp j}^{*2}(-x, t) \right) dx. \quad (24)$$

By requiring the conservation of these quantities, the time derivatives of the norm and the energy lead to the following vertex boundary conditions [32]:

$$\begin{aligned} \gamma_1 q_1(x, t)|_{x=0} &= \gamma_{-1} q_{-1}(x, t)|_{x=0} = \gamma_2 q_2(x, t)|_{x=0} = \gamma_{-2} q_{-2}(x, t)|_{x=0}, \\ \frac{1}{\gamma_1} \partial_x q_1(x, t)|_{x=0} + \frac{1}{\gamma_2} \partial_x q_2(x, t)|_{x=0} &= \frac{1}{\gamma_{-1}} \partial_x q_{-1}(x, t)|_{x=0} + \frac{1}{\gamma_{-2}} \partial_x q_{-2}(x, t)|_{x=0}, \end{aligned} \quad (25)$$

where the parameters $\gamma_{\pm j}$ are non-zero positive real numbers.

Then the solution of the problem given by Eqs. (22) and (25) can be expressed in terms of the solution of Eq. (1) as

$$q_{\pm j}(x, t) = \sqrt{\frac{2}{\beta_{\pm j}}} q(x, t), \quad (26)$$

and it satisfies the boundary conditions (25), provided that the following conditions hold:

$$\frac{\gamma_{\pm j}}{\gamma_{-1}} = \sqrt{\frac{\beta_{\pm j}}{\beta_{-1}}}, \quad \frac{1}{\beta_1} + \frac{1}{\beta_2} = \frac{1}{\beta_{-1}} + \frac{1}{\beta_{-2}}. \quad (27)$$

A traveling soliton solution of Eq. (3) given on a graph can be written as

$$q_{\pm j}(x, t) = \sqrt{\frac{2}{\beta_{\pm j}}} \frac{\alpha_1 e^{-\Delta/2} e^{i(\bar{\xi}_{1R} - \xi_{1R}) + i(\bar{\xi}_{1I} - \xi_{1I})}}{2[\cosh(\chi_1) \cos(\chi_2) + i \sinh(\chi_1) \sin(\chi_2)]}. \quad (28)$$

The sum rule (27) can be considered as a condition (constraint) that ensures the integrability of NNLS equation on a metric star graph given by Eqs. (22) and (25). In other words, if the sum rule (27) is fulfilled, there exist an analytical solution which can be expressed as Eq. (28).

3.2 Derivation of transparent vertex boundary conditions

In this subsection, we derive the TBCs for the nonlocal nonlinear Schrödinger equation on graphs by applying the potential approach used in the derivation of TBCs on a line. Subsequently, the NNLS equation can be formally written as a linear PDE

$$i\partial_t q_{\pm j}(x, t) + \partial_x^2 q_{\pm j}(x, t) + V_{\pm j}(x, t)q_{\pm j}(x, t) = 0, \quad (29)$$

where $V_{\pm j}(x, t) = \sqrt{\beta_j \beta_{-j}} q_{\pm j}(x, t) q_{\mp j}^*(-x, t)$.

Now we split the whole domain (graph) into two subdomains, which we call “interior” (bonds $b_{\pm 1}$) and “exterior” (bonds $b_{\pm 2}$). We use these terminologies to be consistent with those that were used for the problem considered on a line. Moreover, the terminologies are borrowed from the original works [33, 34, 35, 36], in which the basic idea of constructing TBCs was proposed. Accordingly, we consider in the sequel interior and exterior problems. The interior problem for $b_{\pm 1}$ can be written as

$$\begin{aligned} i\partial_t q_{\pm 1} + \partial_x^2 q_{\pm 1} + V_{\pm 1}(x, t)q_{\pm 1} &= 0, \\ q_{\pm 1}|_{t=0} &= Q^I(x), \\ \partial_x q_{\pm 1}|_{x=0} &= \pm(T_0 q_{\pm 1})|_{x=0}, \end{aligned} \quad (30)$$

where $Q^I(x)$ is an initial condition and T_0 is yet an unknown operator that determines the TBCs.

The exterior problems for $b_{\pm 2}$ reads

$$\begin{aligned} i\partial_t q_{\pm 2} + \partial_x^2 q_{\pm 2} + V_{\pm 2}(x, t)q_{\pm 2} &= 0, \\ q_{\pm 2}|_{t=0} &= 0, \\ q_{\pm 2}|_{x=0} &= \psi_{\pm 2}(t), \quad \psi_{\pm 2}(0) = 0, \\ (T_0 \psi_{\pm 2})|_{x=0} &= \mp \partial_x q_{\pm 2}|_{x=0}. \end{aligned} \quad (31)$$

We introduce a new function

$$\mu_{\pm j}(x, t) = e^{-i\nu_{\pm j}(x, t)} q_{\pm j}(x, t), \quad (32)$$

where

$$\nu_{\pm j}(x, t) = \int_0^t V_{\pm j}(x, \tau) d\tau = \sqrt{\beta_j \beta_{-j}} \int_0^t q_{\pm j}(x, \tau) q_{\mp j}^*(-x, \tau) d\tau. \quad (33)$$

Then, the TBCs of the second order approximation (19) for $q_{\pm 2}$ at $x = 0$ can be written as

$$\partial_x q_{\pm 2}|_{x=0} = \pm e^{-i\frac{\pi}{4}} e^{i\nu_{\pm 2}} \cdot \partial_t^{1/2}(e^{-i\nu_{\pm 2}} q_{\pm 2})|_{x=0} \pm i\frac{1}{4} \partial_x V_{\pm 2} e^{i\nu_{\pm 2}} I_t(e^{-i\nu_{\pm 2}} q_{\pm 2})|_{x=0}, \quad (34)$$

where the fractional 1/2-derivative and I_t are given by (20) and (21), correspondingly.

Thus, we find the T_0 operator for $q_{\pm j}$ for $x = 0$ as

$$(T_0 q_{\pm j})|_{x=0} = -e^{-i\frac{\pi}{4}} e^{i\nu_{\pm 2}} \cdot \partial_t^{1/2}(e^{-i\nu_{\pm j}} q_{\pm j})|_{x=0} - i\frac{1}{4} \partial_x V_{\pm j} e^{i\nu_{\pm j}} I_t(e^{-i\nu_{\pm j}} q_{\pm j})|_{x=0}. \quad (35)$$

To find the TBC for $q_{\pm 1}$ at $x = 0$, we apply operator T_0 to $q_{\pm 1}$ as

$$\partial_x q_{\pm 1}|_{x=0} = \mp e^{-i\frac{\pi}{4}} e^{i\nu_{\pm 2}} \cdot \partial_t^{1/2}(e^{-i\nu_{\pm 2}} q_{\pm 2})|_{x=0} \mp i\frac{1}{4} \partial_x V_{\pm 2} e^{i\nu_{\pm 2}} I_t(e^{-i\nu_{\pm 2}} q_{\pm 2})|_{x=0}. \quad (36)$$

From the continuity of the solution in Eq. (25) we have

$$\begin{aligned} \nu_{-1}(0, t) &= \nu_{-2}(0, t) = \nu_1(0, t) = \nu_2(0, t), \\ V_{-1}(0, t) &= V_{-2}(0, t) = V_1(0, t) = V_2(0, t), \\ \sqrt{\beta_{-1}}(T_0 q_{-1})|_{x=0} &= \sqrt{\beta_1}(T_0 q_1)|_{x=0} = \sqrt{\beta_{-2}}(T_0 q_{-2})|_{x=0} = \sqrt{\beta_2}(T_0 q_2)|_{x=0}. \end{aligned} \quad (37)$$

And the current conservation condition in (25) leads to

$$\frac{1}{\sqrt{\beta_{-1}}}(T_0 q_{-1})|_{x=0} + \frac{1}{\sqrt{\beta_1}}(T_0 q_1)|_{x=0} = \frac{1}{\sqrt{\beta_{-2}}}(T_0 q_{-2})|_{x=0} + \frac{1}{\sqrt{\beta_2}}(T_0 q_2)|_{x=0}. \quad (38)$$

Comparing the above Eqs. (37) and (38) gives

$$\frac{1}{\beta_{-1}} + \frac{1}{\beta_1} = \frac{1}{\beta_{-2}} + \frac{1}{\beta_2}. \quad (39)$$

Thus, fulfilling the sum rule (39) implies that the vertex boundary conditions (25) become equivalent to the TBCs at the vertex of the graph. In other words, the vertex becomes “transparent” with respect to soliton transmission. However, since the solution given by Eq. (26) describes a traveling soliton, such “transparency” implies that solitons moving from bonds $b_{\pm 1}$ to bonds $b_{\pm 2}$ transmit through the vertex without any reflection. Such a property can be demonstrated in the numerical experiments presented in the next section. Note that the sum rule (39) is different from the one given by (27) and they coincide only if the parameters $\beta_{\pm j}$ have certain values (for example, if all parameters have the same value, $\beta_{-1} = \beta_1 = \beta_{-2} = \beta_2$, which implies natural boundary conditions). This implies that unlike to the case of classical NLS equation [17, 15], for NNLS equation on metric graphs, integrability is not equivalent to the “transparency” of the vertex.

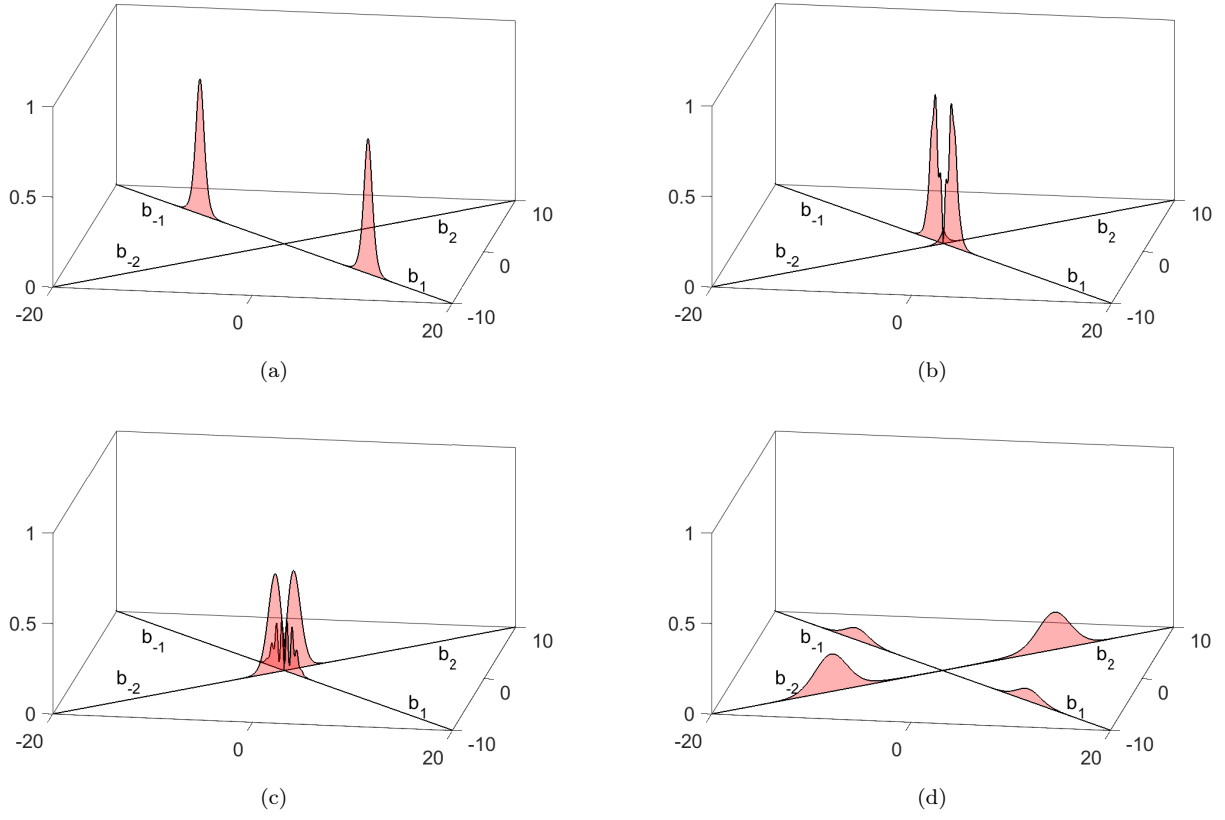


Figure 2: Soliton dynamics at different time moments, i.e., $t = 0$ (a), $t = 0.9$ (b), $t = 1.1$ (c) and $t = 2$ (d) when the sum rule in Eq. (27) is fulfilled by choosing the following values of the nonlinearity coefficients: $\beta_{\pm 1} = 6$ and $\beta_{\pm 2} = 2$.

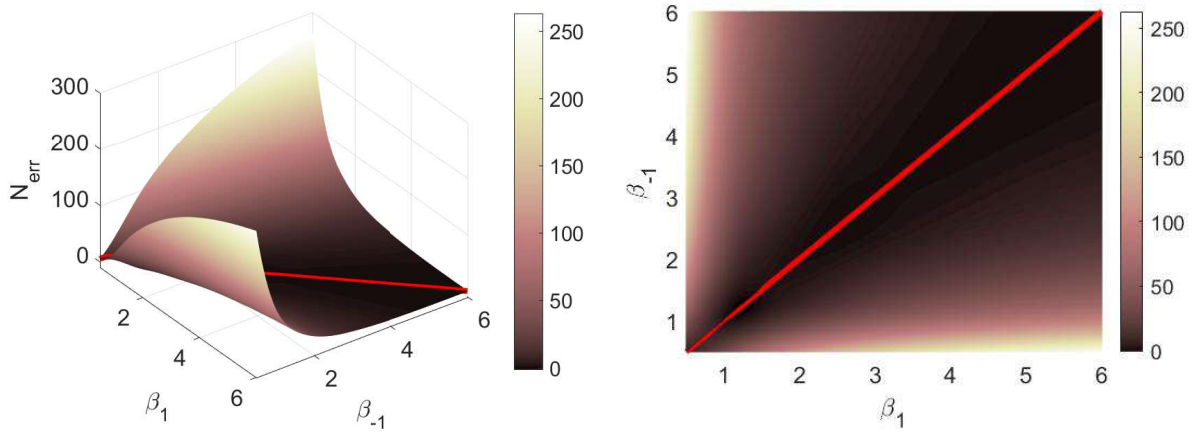


Figure 3: Dependence of the norm conservation on values of parameter β_{-1} and β_1 for fixed $\beta_{-2} = \beta_2 = 2$.

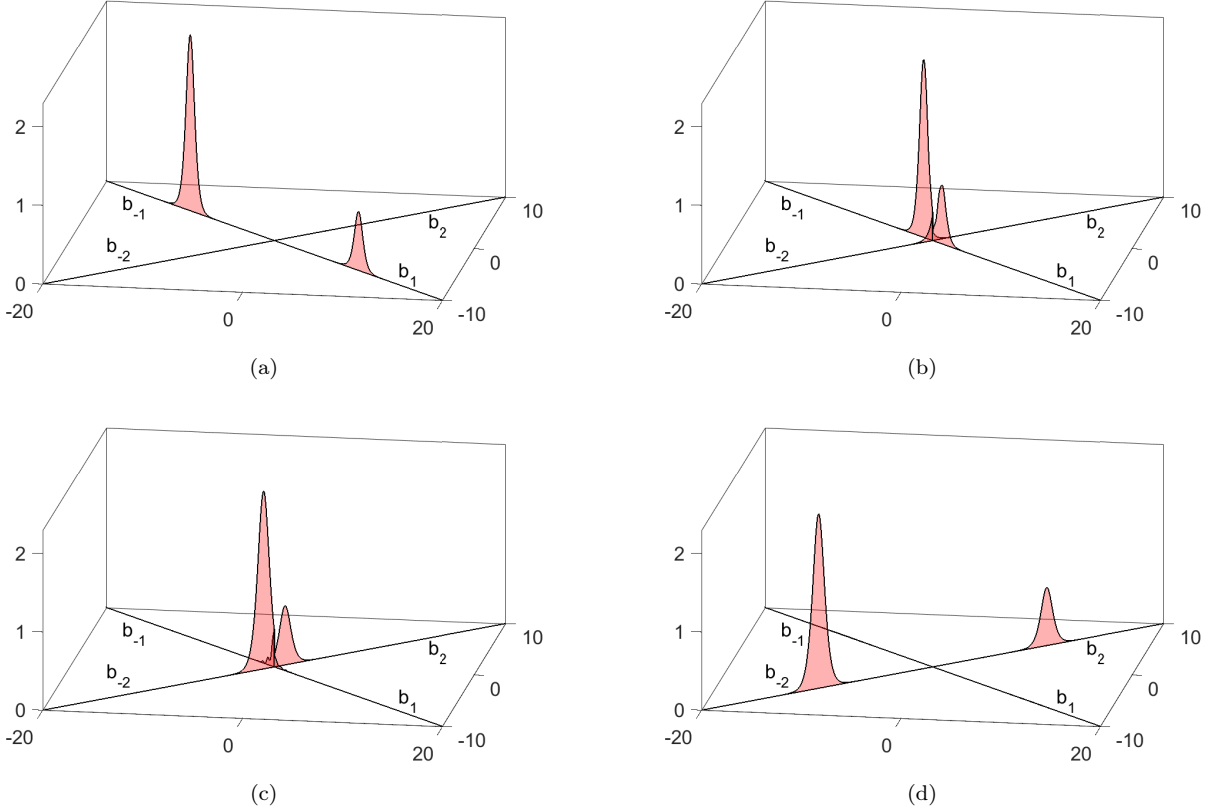


Figure 4: Soliton dynamics at different time moments, i.e., $t = 0$ (a), $t = 0.9$ (b), $t = 1.1$ (c) and $t = 2$ (d) when the sum rule in Eq. (39) is fulfilled by choosing the following values of the nonlinearity coefficients: $\beta_{-1} = \beta_{-2} = 2$ and $\beta_1 = \beta_2 = 6$.

4 Numerical experiment

Here we show the results of a numerical experiment performed to verify the results of deriving transparent vertex boundary conditions (TVBCs) for the nonlocal nonlinear Schrödinger equation on the star graph shown in Fig. 1. In this numerical experiment we use Runge-Kutta method. In all examples we will use the following initial setup: the initial conditions are imposed on b_{-1} and b_1 symmetric bonds and chosen as analytical solutions in Eq. (28), where its parameters are given as $\alpha_1 = 1.13 + 1.13i$, $\beta_1 = 1.13 - 1.13i$ (should not be confused with BC parameters) and $k_1 = \pm 2.5 + 1.5i$, $\bar{k}_1 = \mp 2.5 + 1.5i$ for $b_{\pm 1}$ bonds, respectively.

As a first example we consider the case, when the sum rule (27) is satisfied. The evolution of the traveling solitons for this case is shown in Fig. 2 in four consecutive time steps. This example can be supported by determining the set of parameters pairs (β_{-1}, β_1) for some fixed $\beta_{-2} = \beta_2$. Fig. 3 shows the dependence of the deviation of the norm from its mean as a function of the parameters (β_{-1}, β_1) . In this figure you can see the conservation of the norm along the red line. The deviation of the norm from its mean over the whole time is defined as

$$N_{\text{err}} = \int_0^T |\bar{N} - N| dt, \quad (40)$$

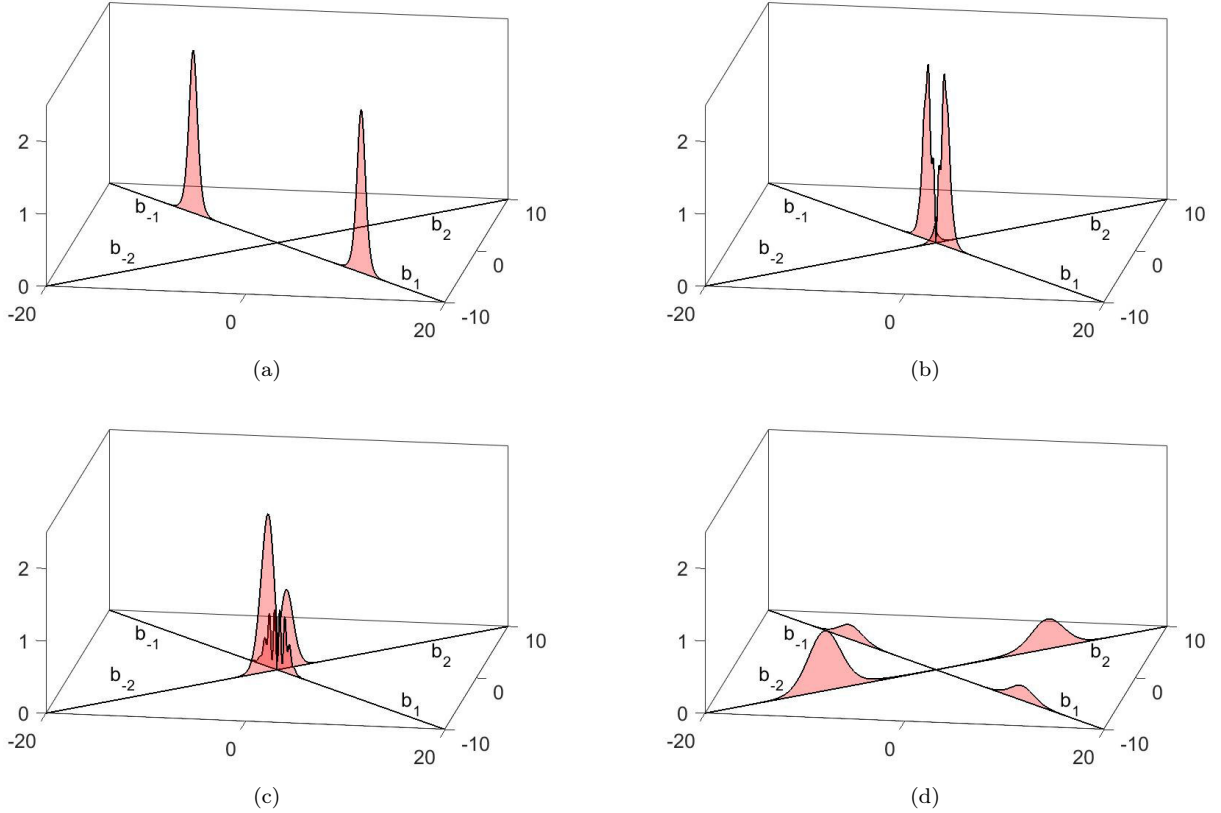


Figure 5: Soliton dynamics at different time moments, i.e., $t = 0$ (a), $t = 0.9$ (b), $t = 1.1$ (c) and $t = 2$ (d) when the sum rules in Eqs. (27) and (39) are broken by choosing the following values of the nonlinearity coefficients: $\beta_{-1} = \beta_1 = 2$ and $\beta_{-2} = 0.5$, $\beta_2 = 1$.

where

$$\bar{N} = \frac{1}{T} \int_0^T N(t) dt$$

is the average value of the total norm over the whole time and T is the total traveling time.

The second example is the case when the sum rule (39) is fulfilled, i.e. when TBCs are imposed at the central vertex. Fig. 4 shows the evolution of the traveling solitons for this case in four consecutive time steps. The reflectionless transmission of the solitons is evident from this plot. As a last example, we consider the case where the sum rule is violated. The results of the calculations are shown in Fig. 5. In this plot one can observe the reflection at the vertex of the graph.

Note that the choice of parameters (β_{-1}, β_1) is obviously not unique for some fixed β_{-2} and β_2 . This can be verified by plotting the dependence of the reflection coefficient on the parameters (β_{-1}, β_1) . For some fixed time instant t_0 , the reflection coefficient can be defined as

$$R = \frac{N_{-1} + N_1}{N_{-1} + N_1 + N_{-2} + N_2}, \quad (41)$$

where $N_{\pm j}$ are partial norms in Eq. (23) of bonds $b_{\pm j}$ at time t_0 . The plot of the reflection coefficient as a function of the BC parameters (β_{-1}, β_1) for fixed $\beta_{-2} = \beta_2 = 2$ at sufficient time ($t = 2$) is shown in Fig. 6. From this plot one can see the black curve (highlighted by the red line) bounded

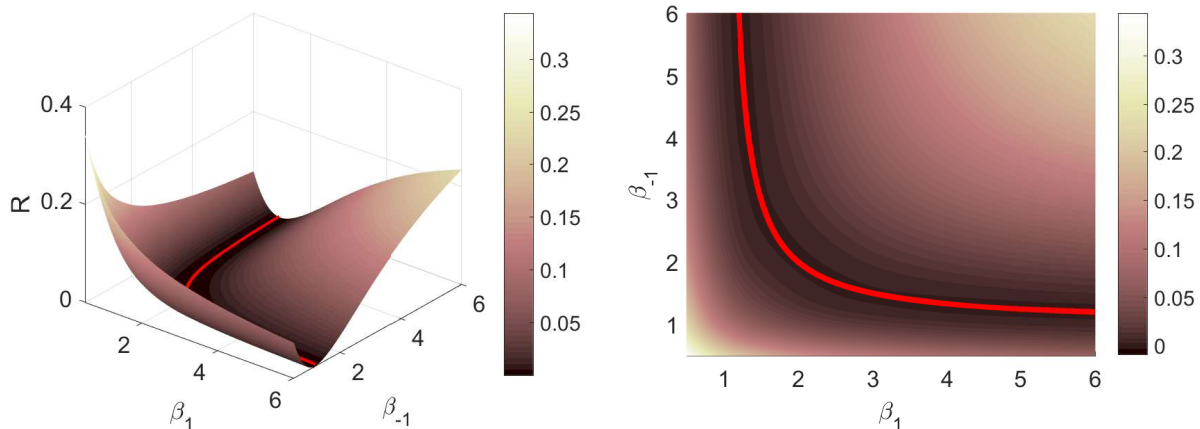


Figure 6: Dependence of the reflection coefficient on values of parameter β_{-1} and β_1 for fixed $\beta_{-2} = \beta_2 = 2$.

by the values of the parameters (β_{-1}, β_1) that satisfy the equation $\beta_{-1}^{-1} + \beta_1^{-1} = 1$. This shows the manifestation of the reflectionless transition of solitons when the constraint (39) is satisfied.

5 Conclusions

In this paper, we have derived transparent boundary conditions for the PT-symmetric nonlocal nonlinear Schrödinger equation on metric graphs using the so-called potential approach. Constraints that make transparent boundary conditions to weight-continuity and generalized Kirchhoff conditions are derived. Numerical utilization of transparent boundary conditions and numerical proof of their equivalence to weight-continuity and generalized Kirchhoff rules are provided. For PT-symmetric solitons, the transparency implies the reflectionless transmission of a “wing” of the soliton from the bond $b_{\pm 1}$ to the bond $b_{\pm 2}$. The results obtained in this work can be applied to the modeling of optical networks and optoelectronic devices using PT-symmetric solitons, so that the minimum signal loss can be achieved by tuning the soliton propagation.

Acknowledgment

The work is supported by the grant of the Agency for innovative development under the Ministry of higher education, science and innovation of the Republic of Uzbekistan (Ref. No. F-2021-440) and by the Grant REP-04032022/206, funded under the MUNIS Project, supported by the World Bank and the Government of the Republic of Uzbekistan.

References

- [1] M.J. Ablowitz and Z.H. Musslimani, Phys. Rev. Lett. **110**, 064105 (2013).
- [2] M.J. Ablowitz and Z.H. Musslimani, Phys. Rev. E **90**, 032912 (2014).
- [3] M.J. Ablowitz and Z.H. Musslimani, Nonlinearity **29**, 915 (2016).

- [4] M.J. Ablowitz and Z.H. Musslimani, *Stud. Appl. Math.* **139**, 7 (2016).
- [5] B-F. Feng, X-D. Luo, M.J. Ablowitz, and Z.H. Musslimani, *Nonlinearity* **31**, 5385 (2018).
- [6] M.J. Ablowitz, X-D. Luo, and Z.H. Musslimani, *J. Math. Phys.* **59**, 011501 (2018).
- [7] M.J. Ablowitz, Z.H. Musslimani, *J. Phys. A* **52**, 15LT02 (2019).
- [8] S. Stalin, M. Senthilvelan, and M. Lakshmanan, *Phys. Lett. A* **381**, 2380 (2017).
- [9] Z. Wen and Zh. Yan, *Chaos* **27**, 053105 (2017).
- [10] J. Yang, *Phys. Rev. E* **98**, 042202 (2018).
- [11] D. Sinha and P.K. Ghosh, *Phys. Rev. E* **91**, 042908 (2015).
- [12] R. Rusin, R. Kusdiantara, and H. Susanto, *Phys. Lett. A* **383**, 2039 (2019).
- [13] Z. Wen and Zh. Yan, *Chaos* **27**, 053105 (2017).
- [14] O. Maor, N. Dror, and B.A. Malomed, *Opt. Lett.* **38**, 5454-5457 (2013).
- [15] J.R. Yusupov, K.K. Sabirov, M. Ehrhardt, and D.U. Matrasulov, *Phys. Rev. E* **100**, 032204 (2019).
- [16] R. Adami, C. Cacciapuoti, D. Finco, D. Noja, *Rev. Math. Phys.* **23**, 4 (2011).
- [17] Z. Sobirov, D. Matrasulov, K. Sabirov, S. Sawada, and K. Nakamura, *Phys. Rev. E* **81**, 066602 (2010).
- [18] D. Noja, *Philos. Trans. R. Soc. A* **372**, 20130002 (2014).
- [19] D. Noja, D. Pelinovsky, and G. Shaikhova, *Nonlinearity* **28**, 2343 (2015).
- [20] R. Adami, C. Cacciapuoti, D. Noja, *J. Diff. Eq.* **260**, 7397 (2016).
- [21] V. Caudrelier, *Comm. Math. Phys.* **338**, 893 (2015).
- [22] R. Adami, E. Serra, P. Tilli, *Commun. Math. Phys.* **352**, 387 (2017).
- [23] A. Kairzhan, D.E. Pelinovsky, *J. Phys. A: Math. Theor.* **51**, 095203 (2018).
- [24] J.R. Yusupov, Kh.Sh. Matyokubov, K.K. Sabirov, and D.U. Matrasulov, *Chem. Phys.* **537**, 110861 (2020).
- [25] D. Matrasulov, K. Sabirov, D. Babajanov, and H. Susanto, *EPL* **130**, 67002 (2020).
- [26] K.K. Sabirov, M.E. Akramov, R. Sh. Otajonov, and D.U. Matrasulov, *Chaos, Solitons & Fractals* **133**, 109636 (2020).
- [27] M.E. Akramov, J.R. Yusupov, M. Ehrhardt, H. Susanto, and D.U. Matrasulov, *Phys. Lett. A* **459**, 128611 (2023).
- [28] X. Antoine, Ch. Besse, and S. Descombes, *SIAM J. Numer. Anal.* **43**, 2272 (2006).

- [29] K.K. Sabirov, J.R. Yusupov, M.M. Aripov, M. Ehrhardt, and D.U. Matrasulov, Phys. Rev. E **103**, 043305 (2021).
- [30] K. K. Sabirov, J. R. Yusupov, M. Ehrhardt, D. U. Matrasulov. Phys, Lett. A **423**, 127822 (2021).
- [31] M. Taylor, Pseudo Differential Operators, Springer, 2006.
- [32] M. Akramov, K. Sabirov, D. Matrasulov, H. Susanto, S. Usanov, and O. Karpova, Phys. Rev. E **105**, 054205 (2022).
- [33] M. Ehrhardt, VLSI Design **9(4)**, 325 (1999).
- [34] M. Ehrhardt and A. Arnold, Riv. di Math. Univ. di Parma **6(4)**, 57 (2001).
- [35] A. Arnold, M. Ehrhardt, and I. Sofronov, Commun. Math. Sci. **1(3)**, 501 (2003).
- [36] X. Antoine, A. Arnold, C. Besse, M. Ehrhardt, and A. Schädle, Commun. Comput. Phys. **4(4)**, 729 (2008).